THERMAL AND RHEOLOGICAL CHARACTERISATION OF PLA COMPOSITES WITH LIGNOCELLULOSIC ADDITIVES

[1]Mariia KOSTENKO, [2,3]Lucie ZARYBNICKA, [4]Yurij STETSYSHYN, [1] Milan KRACALIK

[1]Johannes Kepler University Linz, Institute of Polymer Science, Altenberger Str. 69, 4040 Linz, Austria, EU, mariia.kostenko@jku.at, Milan.Kracalik@jku.at

[2]Department of Technical Studies, College of Polytechnics Jihlava, Tolsteho 16, 586 01Jihlava, Czech Republic, EU, Lucie.Zarybnicka@vspj.cz

[3]Institute of Theoretical and Applied Mechanics of the Czech Academy of Sciences, Prosecka 809/76, 190 00 Prague 9, Czech Republic, EU, Lucie.Zarybnicka@vspj.cz

[4]Lviv Polytechnic National University, 3/4 St. Yura Square, 79013 Lviv, Ukraine, yrstecushun@ukr.net

https://doi.org/10.37904/nanocon.2025.5172

Abstract

This study examines the rheological properties and technological characteristics of five types of AzureFilm filament made from polylactic acid (PLA), modified with three kinds of wood fillers (bamboo, pine, and cork), as well as poly(p-phenylene pyromellitimide) (PPPI). The filaments underwent multiple processing steps, including grinding, drying, and melting, followed by injection molding. The rheological properties of the composites were measured in the molten state using a rotational rheometer at 210 °c. Notably, Cole–Cole and Van Gurp–Palmen (VGP) plots were created to analyze relaxation behavior, polydispersity, and interfacial interaction. Furthermore, thermal transitions and degradation were studied using differential scanning calorimetry (DSC) and thermogravimetric analysis (TGA), providing insights into the comparative effects of natural lignocellulosic fillers and a high-performance aromatic additive.

Keywords: Polylactic acid (PLA); rheology; biopolymer composites; thermoplastic processing; viscoelastic behavior

1. INTRODUCTION

Polylactic acid (PLA) is a biodegradable thermoplastic widely used in applications such as packaging and disposable goods due to its biocompatibility, renewability, and ability to degrade under industrial composting conditions [1,2]. Its growing use in additive manufacturing is driven by its low processing temperature and ease of printing. However, limitations in thermal resistance and mechanical toughness restrict its use in high-performance applications [3]. To address these issues, various bio-based fillers such as wood, bamboo, and cork have been introduced as reinforcements to improve stiffness, crystallinity, and thermal behavior [4–7]. These lignocellulosic fillers, composed mainly of cellulose, hemicellulose, and lignin, interact with the PLA matrix through heterogeneous nucleation and physical entanglement [6]. Similar rheological approaches have been successfully used to evaluate micro- and nano-structured systems, including recycled clay/polyethylene terephthalate nanocomposites [8]. This demonstrates the power of rheology in probing structure and property evolution.

Their morphological diversity and chemical complexity significantly influence filler–matrix adhesion, crystallization dynamics, and melt behavior. Nevertheless, their inherent variability and relatively large particle dimensions often lead to incomplete dispersion and inconsistent composite properties [9, 10].

To overcome these drawbacks, this study also includes PLA modified with 5% poly(p-phenylene pyromellitimide) (PPPI) - a nanostructured aromatic polyimide synthesized via hydrothermal polymerization

[11, 12]. Unlike natural fillers, PPPI forms uniformly dispersed nano-scale spherical particles, enabling intimate interaction with the PLA matrix. Incorporating PPPI provides a valuable contrast: lignocellulosic fillers represent microstructured, bio-based reinforcements, whereas PPPI offers a nanostructured, synthetic alternative. This distinction allows a direct comparison of reinforcement mechanisms across structural scales, highlighting how filler size, morphology, and chemistry influence melt rheology, crystallization, and thermal degradation [13, 14].

Accordingly, the present work investigates the thermal and rheological characteristics of PLA composites with three lignocellulosic fillers (bamboo, pine, cork) and nanostructured PPPI, using thermogravimetric analysis (TGA), differential scanning calorimetry (DSC), and rotational rheometry. Structural insights were further obtained through Cole–Cole and Van Gurp–Palmen (VGP) analyses to assess relaxation dynamics and filler–matrix interactions [8, 15-18].

2. MATERIALS AND METHODS

2.1 Characterization of filaments

This study investigated five types of PLA-based filament. Four of these were supplied by AzureFilm: pure PLA (PLA Transparent) and three PLA composites containing approximately 40 wt.% of lignocellulosic fillers derived from pine, cork and bamboo (see **Table 1**). The filler content and nature are known to influence melt behavior due to differences in morphology and interfacial interactions [4, 6, 12, 15].

Table 1 General information on the material

Filament Name	Matrix	Filler	Diameter	Recommended Extrusion (°)	Bed, (°)
PLA Transparent	PLA	—	1.75 mm	200–230 °C	60 °C
3d Wood Pine	PLA	Wood (pine), 40%	1.75 mm	200–230 °C	60 °C
3d Wood Cork	PLA	Wood (cork), 40%	1.75 mm	200–230 °C	60 °C
3d Wood Bamboo	PLA	Wood (bamboo), 40%	1.75 mm	200–230 °C	60 °C
PLA+PPPI	PLA	5% PPPI	-	200–230 °C	-

The fifth material, PLA with 5 wt% PPPI, was synthesized at TU Wien, Institute of Materials Chemistry. PPPI is a thermally stable aromatic polyimide produced via hydrothermal polymerization to form nano-scale spherical domains with high dispersibility. This sample was included to contrast the effect of nanostructured fillers with that of traditional, micro-sized lignocellulosic additives.

2.2 Sample Preparation

Following established methodologies [9, 10], all commercial filaments were cut into 3–5 mm granules and dried at 60 °C for 12 h to minimize hydrolytic degradation during melt processing. The granules were homogenized using a Haake MiniLab twin-screw micro-compounder, after which disk-shaped specimens (25 mm diameter) were injection-molded with a Haake MiniJet system. This ensured a consistent processing history across all samples, in line with previous work on fibre-filled PLA composites [14, 16].

For PLA+5%PPPI, neat PLA pellets were melt-compounded with PPPI powder (5 wt%) before injection molding. The identical processing route enabled a fair comparison between microstructured natural fillers and the nanostructured synthetic additive.

2.3 Analysis

To analyze the samples used, methods such as thermogravimetric analysis (TGA), Dynamic Scanning Calorimetry (DSC), and rotary rheometry (rheological properties) were employed.

2.3.1 Thermogravimetric analysis (TGA)

TGA was performed on samples of approximately 10 mg under a nitrogen atmosphere, at a heating rate of 10 °C/min, from 25 to 600 °C, following established protocols for PLA composites [6, 15, 19].

2.3.2 Differential scanning calorimetry (DSC)

DSC analysis was performed from 0 to 220 °C at a heating rate of 10 °C/min under a nitrogen purge. The data were used to determine the Tg, Tc and Tm values. The methodology was consistent with that used in prior studies on PLA and PLA–fibre composites [5, 12, 16].

2.3.3 Rheological measurements

Dynamic rheological tests were performed using a rotational rheometer with parallel plate geometry (25 mm diameter) at 210 °C. Frequency sweeps were conducted from 0.1 to 628 rad/s, maintaining a strain amplitude within the linear viscoelastic region. The data were then used to construct plots of complex viscosity, storage modulus (G′), Cole–Cole, and Van Gurp–Palmen (VGP) plots, as reported in previous studies [8, 14-15, 17-18, 20].

3. RESULTS AND DISCUSSION

3.1 Thermal properties of PLA nanocomposites

Thermogravimetric analysis (TGA, **Figure 1a**) showed single-step degradation for all systems. Neat PLA started to decompose at around 330 °C, consistent with previous studies [7, 12, 19]. Wood-filled composites exhibited slightly lower onset degradation temperatures (326–330 °C) due to the reduced stability of hemicellulose and lignin, but higher char residue levels (1–2%), indicating biochar formation from lignin decomposition [12, 15].

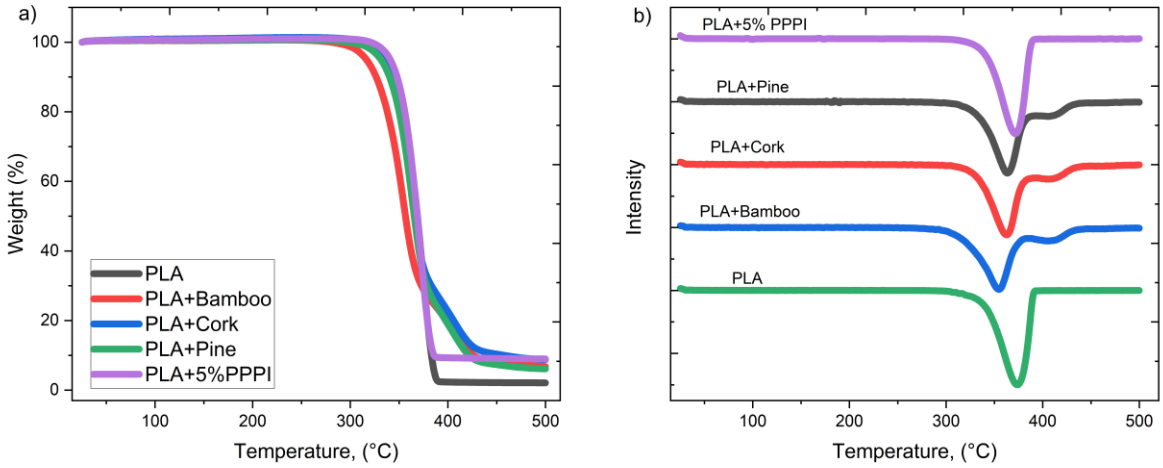

Figure 1 TGA (a) and DTG (b) for PLA-based nanocomposite

The PLA+5%PPPI composite showed the highest onset temperature (335 °C) and maximum degradation temperature (371 °C), exceeding both neat PLA and wood-based composites. Additionally, the residual char yield reached approximately 3.5%, due to the thermally stable aromatic backbone of the polyimide [11, 21]. Derivative thermogravimetry (DTG, Figure 1b) confirmed this trend, displaying a narrower degradation peak for PPPI compared to the broader multi-step behavior of the wood composites.

Table 2 Thermogravimetric characteristics and thermal transition temperature (from DSC) of PLA and PLA-based composites

Sample	Tg, (°C)	Tc, (°C)	Tm, (°C)	Temp. at 10 % Mass Loss (°C)	Onset Degradation (°C)	Max. Degradation Temp. (°C)	Residual Mass at 500 °C (%)
PLA	61,92	-	150,0	294	331	368	0,3
PLA+Bamboo	60,88	111,46	147,33	273	326	361	1,3
PLA+Pine	61,34	116,20	148,84	285	328	362	2,0
PLA+Cork	61,45	115,86	148,84	287	330	364	1,0
PLA+5%PPPI	62,0	113,0	149,0	301	335	371	3,5

Figure 2 and **Table 2** present the differential scanning calorimetry (DSC) curves and their main values, illustrating three key transitions: the glass transition (Tg), crystallization (Tc), and melting (Tm). Pure PLA shows a glass transition temperature (Tg) of approximately 62 °C but no crystallization peak, confirming its poor nucleating ability and slow crystallization kinetics [2, 5, 12]. Conversely, wood-filled composites display well-defined crystallization peaks. Bamboo-filled PLA exhibits the lowest crystallization temperature (Tc ≈ 111 °C) and a broader melting transition (Tm ≈ 147 °C), indicating its partial crystallinity and decreased structural order. Pine and cork fillers result in higher Tc values (around 115–116 °C), with pine producing the sharpest crystallization exotherm, which aligns with their heterogeneous nucleating effect [6, 15, 16].

PLA+5%PPPI showed an intermediate crystallization temperature (Tc ≈ 113 °C) and a sharply defined melting peak (Tm ≈ 149 °C). This behavior indicates that PPPI acts as a moderate nucleating agent, allowing crystalline packing while maintaining a uniform dispersion of nanospheres. This contrasts with lignocellulosic fillers, showing that nanoscale PPPI reinforcement balances crystallinity with improved stability [11].

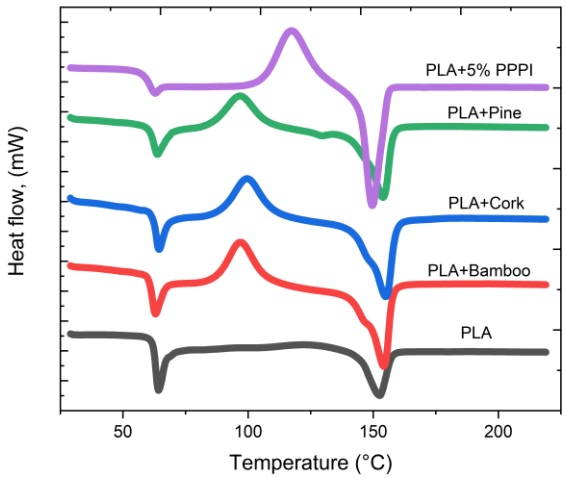

Figure 2 DSC for PLA-based nanocomposite

3.2 Complex Viscosity (η*)

Figure 3(a) shows that all PLA-based systems displayed shear-thinning behavior, with the complex viscosity (η*) decreasing as the frequency increased, as is typical of PLA melts [3, 5, 14]. Among the composites, cork-filled PLA exhibited the highest viscosity at low frequencies, reflecting strong interactions between the filler and the matrix, as well as the formation of a network-like structure [6, 13]. Bamboo composites showed the least viscosity enhancement, remaining close to that of neat PLA.

PLA+5%PPPI showed an intermediate viscosity, higher than that of neat PLA and bamboo but lower than cork. This indicates that adding PPPI encouraged moderate structuring of the melt, aligning with nanoscale reinforcement improving chain entanglement without creating excessive heterogeneity [11, 21].

3.3 Storage modulus (G')

As shown in **Figure 3(b)**, the storage modulus (G′) of PLA and its composites increased with angular frequency, indicating the viscoelastic behavior typical of polymer melts [3, 14]. All lignocellulosic composites displayed higher G′ values than pure PLA, implying greater stiffness and partial formation of an elastic network. Cork showed the most significant increase, probably due to stronger interfacial adhesion and a more interconnected microfibrillar structure [6, 15, 16]. In contrast, bamboo-based PLA demonstrated only minor reinforcement and remained closest to neat PLA, aligning with weaker filler–matrix interactions [12].

The PLA+5%PPPI composite also showed a higher storage modulus than neat PLA, although it was lower than that of cork. This intermediate behavior indicates that the presence of PPPI nanodomains limits chain mobility and adds extra elastic reinforcement, which aligns with the rigid aromatic structure of polyimides [11, 21].

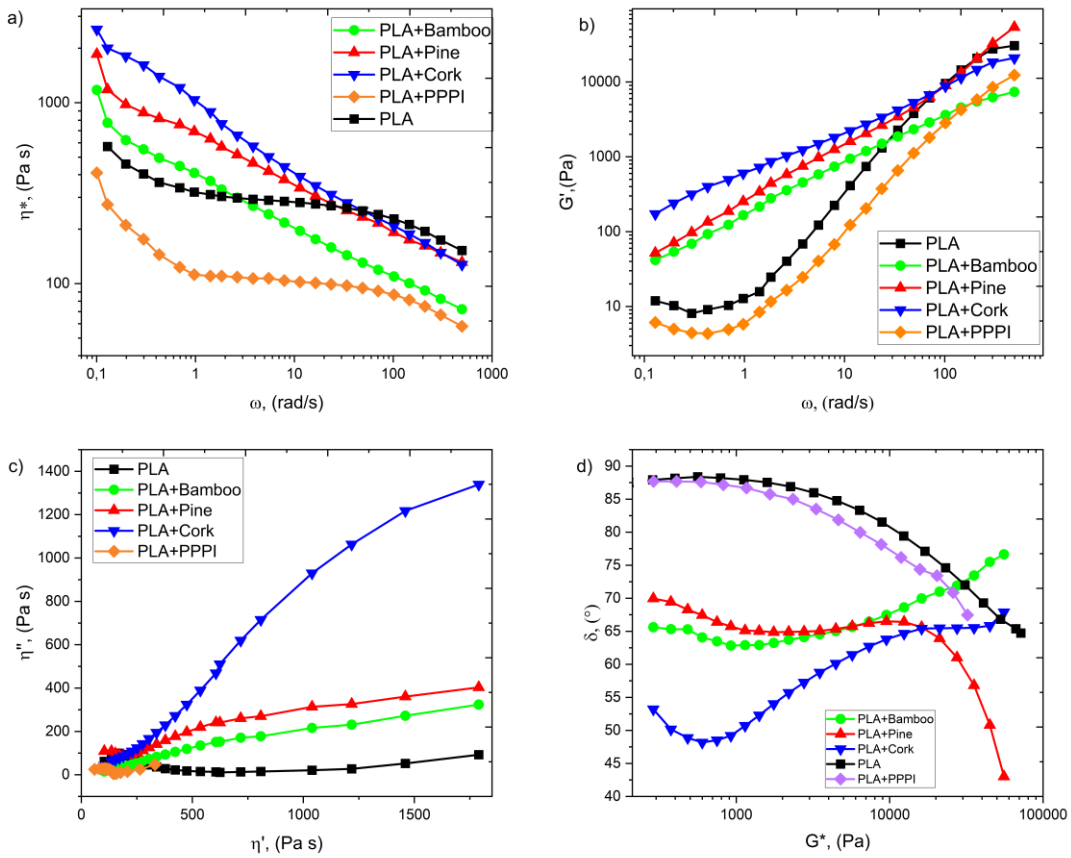

Figure 3 Dependence of the complex viscosity on the angular frequency (a); Dependence of the storage module (G´) (b); Van Gurp-Palmen diagram (c); Cole-Cole diagram (d).

3.4 Cole-Cole diagram

The Cole–Cole plot (**Figure 3c**) compares the imaginary (η″) and real (η′) parts of the complex viscosity, providing insights into relaxation dynamics [14, 18]. Neat PLA displayed a near semicircular profile, consistent with homogeneous amorphous polymers with a relatively narrow molecular weight distribution [16].

Cork-filled PLA showed the greatest upward deviation, reflecting strong filler–matrix friction and limited chain relaxation [6,18]. Pine composites displayed intermediate behavior with irregular arcs, while bamboo composites resembled neat PLA more closely, indicating limited structural organization.

PLA+5%PPPI showed a moderate deviation above neat PLA, similar to the cork composite but less noticeable. This indicates improved interfacial interaction and energy dissipation, which aligns with the formation of nanoscale microdomains within the PLA matrix [11, 21].

3.5 Van Gurp-Palmen analysis

The VGP plot (**Figure 3d**) shows the phase angle (δ) as a function of the complex modulus magnitude (|G*|). Neat PLA exhibited phase angles close to 90° at low |G*|, indicating viscous-dominated behavior [14, 20]. Cork reduced δ most significantly, reflecting the formation of a network-like structure and increased elastic response [6, 15]. Pine composites showed moderate reinforcement, whilst bamboo composites remained close to the properties of neat PLA.

PLA+5%PPPI also decreased δ compared to neat PLA, though less significantly than cork. This suggests that PPPI nanospheres improved melt elasticity and encouraged partial network formation, strengthening the PLA matrix through nanoscale aromatic domains [11, 21].

CONCLUSION

Overall, the study demonstrates that the reinforcement mechanisms in PLA-based composites depend strongly on the filler's structure and chemistry. Microstructured lignocellulosic fillers - bamboo, pine, and cork mainly acted as heterogeneous nucleating agents, moderately influencing crystallization behavior, thermal stability, melt viscosity, and storage modulus. Among these fillers, cork and pine produced the most significant enhancements in nucleation efficiency, viscosity, and G′, while bamboo showed the weakest effect, suggesting weaker filler–matrix interactions and rheological behavior closest to neat PLA. Cole–Cole and VGP analyses confirmed these trends, with cork exhibiting increased internal friction and reduced phase angles, and bamboo showing relaxation behavior similar to pure PLA.

Thermal analyses further revealed structural differences among the natural fillers. Pine and cork generated higher crystallization temperatures and sharper melting peaks, while bamboo acted as a poorer nucleator. All composites displayed single-step degradation around 330 °C, but cork composites retain the highest residue among natural fillers.

In contrast to the microstructured fillers, the nanostructured PPPI additive operated through a distinct reinforcement mechanism. PPPI enhanced both thermal stability and rheological performance by increasing the onset degradation temperature (up to 335 °C), maximum degradation temperature (371 °C), and char residue (~3.5%). DSC analysis showed moderate nucleation without disrupting crystalline order. Rheological measurements demonstrated increased melt elasticity and viscosity, reflected in elevated G′ and reduced δ in VGP analysis. These effects correlate with the formation of stable aromatic nanoscale domains and improved filler–matrix interactions at the nanoscale.

Taken together, microstructured natural fillers primarily contributed to nucleation and crystallinity, while PPPI provided nanoscale reinforcement that enhanced thermal resistance and melt elasticity. Cork emerged as the most reinforcing and thermally stabilizing natural filler, whereas bamboo functioned mainly as a dispersed, weakly interacting phase. PPPI offered complementary benefits at low loading, combining thermal stabilization with rheological reinforcement.

These combined micro–nano insights underscore the importance of integrating thermal and rheological analyses when designing advanced PLA-based composites. They highlight the potential of hybrid strategies

that combine microstructured bio-based fillers with nanostructured synthetic additives to achieve customized performance in next-generation bio-based thermoplastics.

ACKNOWLEDGEMENTS

We want to express our gratitude for the financial support provided by the LIT Institute of Technology at Johannes Kepler University Linz, project number: LIT-2022-11-SEE-123

REFERENCES

[1] MAZUR, K.E., BORUCKA, A., KACZOR, P. *et al.* Mechanical, Thermal and Microstructural Characteristic of 3D Printed Polylactide Composites with Natural Fibers: Wood, Bamboo and Cork. *J Polym Environ.* 2022, vol. 30, pp. 2341–2354. Available from: https://doi.org/10.1007/s10924-021-02356-3

[2] PLAMADIALA, I., CROITORU, C., POP, M. A., & ROATA, I. C. (2025). Enhancing Polylactic Acid (PLA) Performance: A Review of Additives in Fused Deposition Modelling (FDM) Filaments. *Polymers*. 2025, vol. 17, no. 2, 191. Available from: https://doi.org/10.3390/polym17020191

[3] GUPTA, A.; SIMMONS, W.; SCHUENEMAN, G. T.; HYLTON, D.; MINTZ, E. A. Rheological and Thermo-Mechanical Properties of PLA/Lignin-Coated Cellulose Nanocrystal Composites. *ACS Sustainable Chem. Eng.* 2017, vol. 5, no. 2, pp. 1711–1720. Available from: https://doi.org/10.1021/acssuschemeng.6b02458

[4] SCAFFARO, R.; et al. *Lignocellulosic Fillers and Graphene Nanoplatelets for PLA Reinforcement.* Compos. Sci. Technol. 2020, vol. 190, 108008. Available from: https://doi.org/10.1016/j.compscitech.2020.108008

[5] ALTUNTAS, Ertugrul, & AYDEMIR, Deniz. Effects of wood flour on the mechanical, thermal and morphological properties of poly (L-lactic acid)-chitosan biopolymer composites. *Maderas. Ciencia y tecnología*. 2019, vol. 21, no. 4, pp. 611-618. Available from: https://dx.doi.org/10.4067/S0718-221X2019005000416

[6] NIANG, B.; et al. *Rheological Properties of PLA–Typha Based Biocomposites.* OJCM. 2021, vol. 11, no. 4, pp. 111–122. Available from: https://doi.org/10.4236/ojcm.2021.114009

[7] NATARAJ G, RAMESH BABU S. Enhancing mechanical properties of PLA-based bio composite filament reinforced with horse gram filler for 3D printing applications. *J Vinyl Addit Technol*. 2025; vol. 31, no. 2, pp. 453-468. Available from: https://doi.org/10.1002/vnl.22182

[8] M. KOSTENKO, Y. STETSYSHYN, K. HARHAY, Y. MELNYK, V. DONCHAK, Z. GUBRIY, M. KRACALIK, *J. Appl. Polym. Sci.* 2024, vol. 141, no. 25, e55543. Available from: https://doi.org/10.1002/app.55543

[9] DEJENE B.K., GUDAYU A.D. Achieving performance and functionality in PLA-based packaging: Insights from hybrid composites with false banana (Enset) fiber and ZnO nanoparticles. *Journal of Thermoplastic Composite Materials*. 2024, vol. 38, no. 6, pp. 2138-2168. Available from: https://doi.org/10.1177/08927057241288125

[10] PARK, I. H., LEE, J. Y., AHN, S. J., & CHOI, H. J. (2020). Melt Rheology and Mechanical Characteristics of Poly(Lactic Acid)/Alkylated Graphene Oxide Nanocomposites. *Polymers*. 2020, vol.12, no. 10, 2402. Available from: https://doi.org/10.3390/polym12102402

[11] R. SALEHIYAN, S.S. RAY. *Macromol. Mater. Eng.* 2018, 303, 1800134. Available from: https://doi.org/10.1002/mame.201800134

[12] BARCZEWSKI, M.; MYSIUKIEWICZ, O. Rheological and Processing Properties of Poly(lactic acid) Composites Filled with Chestnut Shell. *Polymer Korea*. 2018, vol. 42, no. 2, pp. 267-274. Available from: https://doi.org/10.7317/pk.2018.42.2.267

[13] IVANOVA, R.; KOTSILKOVA, R. Rheological study of poly(lactic) acid nanocomposites with carbon nanotubes and graphene additives as a tool for materials characterization for 3D printing application. *Appl. Rheol*. 2018, vol. 28, 54014. Available from: https://doi.org/10.3933/applrheol-28-54014

[14] SALEHIYAN, R., SOLEYMANI EIL BAKHTIARI, S. A review on rheological approaches as a perfect tool to monitor thermal degradation of biodegradable polymers. *Korea-Aust. Rheol. J.* 2024, vol. 36, pp. 295–317. Available from: https://doi.org/10.1007/s13367-024-00111-3

[15] Milan KRACALIK. Rheology of multiphase polymer systems using novel “melt rigidity” evaluation approach. *AIP Conf. Proc.* 28 April 2015; vol. 1662, no. 1, 040002. Available from: https://doi.org/10.1063/1.4918890

[16] ZÁRYBNICKÁ, L., MACHOVÁ, D. and DVOŘÁK, K. "Effect of copper or carbon fiber addition to the 3D printing of polylactid samples" *Materials Testing*. 2020, vol. 62, no. 7, pp. 727-732. Available from: https://doi.org/10.3139/120.111543.

[17] SHARIF, A., MONDAL, S., HOQUE, M.E. (2019). Polylactic Acid (PLA)-Based Nanocomposites: Processing and Properties. In: Sanyang, M., Jawaid, M. (eds) Bio-based Polymers and Nanocomposites. Springer, Cham. Available from: https://doi.org/10.1007/978-3-030-05825-8_11

[18] FERRI, J. M.; et al. *PLA with Lignocellulosic Byproducts.* Ind. Crops Prod. 2016, vol. 95, pp. 582–590.

[19] JUBINVILLE, D.; TZOGANAKIS, C.; MEKONNEN, T. H. Recycled PLA–Wood Flour Based Biocomposites: Effect of Wood Flour Surface Modification, PLA Recycling, and Maleation. *Construction and Building Materials.* 2022, vol. 352, 129026. Available from: https://doi.org/10.1016/j.conbuildmat.2022.129026

[20] MOFOKENG J.P., LUYT A.S., TÁBI T., KOVÁCS J. Comparison of injection moulded, natural fibre-reinforced composites with PP and PLA as matrices. *Journal of Thermoplastic Composite Materials*. 2012, vol. 25, no. 8, pp. 927-948. Available from: https://doi.org/10.1177/0892705711423291

[21] ZHANG, Q.; MA, L.; ZHANG, X.; ZHANG, L.; WANG, Z. Lignocellulose nanofiber/polylactic acid (LCNF/PLA) composite with internal lignin for enhanced performance as 3D printable filament. *Industrial Crops and Products* 2022, vol. 178, 114590. Available from: https://doi.org/10.1016/j.indcrop.2022.114590